Available online at www.sciencedirect.com
SCIENCE DIRECT
Biochimica et Biophysica Acta 1712 (2005) 137 – 151
BIOCHIMICA ET BIOPHYSICA ACTA
BBA
http://www.elsevier.com/locate/bba

# Premicellar complexes of sphingomyelinase mediate enzyme exchange for the stationary phase turnover

Bao-Zhu Yu[a], Tatyana Polenova[a,*], Mahendra Kumar Jain[a,*], Otto G. Berg[b,*]

[a]*Department of Chemistry and Biochemistry, University of Delaware, Newark, DE 19716, USA*
[b]*Department of Molecular Evolution, Uppsala University Evolutionary Biology Center, Uppsala, Sweden*

Received 27 January 2005; received in revised form 18 March 2005; accepted 24 March 2005
Available online 15 April 2005

**Abstract**

During the steady state reaction progress in the scooting mode with highly processive turnover, *Bacillus cereus* sphingomyelinase (SMase) remains tightly bound to sphingomyelin (SM) vesicles (Yu et al., Biochim. Biophys. Acta 1583, 121–131, 2002). In this paper, we analyze the kinetics of SMase-catalyzed hydrolysis of SM dispersed in diheptanoylphosphatidyl-choline ($DC_7PC$) micelles. Results show that the resulting decrease in the turnover processivity induces the stationary phase in the reaction progress. The exchange of the bound enzyme (E*) between the vesicle during such reaction progress is mediated via the premicellar complexes ($E_i^{\#}$) of SMase with $DC_7PC$. Biophysical studies indicate that in $E_i^{\#}$ monodisperse $DC_7PC$ is bound to the interface binding surface (i-face) of SMase that is also involved in its binding to micelles or vesicles. In the presence of magnesium, required for the catalytic turnover, three different complexes of SMase with monodisperse $DC_7PC$ ($E_i^{\#}$ with $i=1, 2, 3$) are sequentially formed with Hill coefficients of 3, 4 and 8, respectively. As a result, during the stationary phase reaction progress, the initial rate is linear for an extended period and all the substrate in the reaction mixture is hydrolyzed at the end of the reaction progress. At low mole fraction ($X$) of total added SM, exchange is rapid and the processive turnover is limited by the steps of the interfacial turnover cycle without becoming microscopically limited by local substrate depletion or enzyme exchange. At high $X$, less $DC_7PC$ will be monodisperse, $E_i^{\#}$ does not form and the turnover becomes limited by slow enzyme exchange. Transferred NOESY enhancement results show that monomeric $DC_7PC$ in solution is in a rapid exchange with that bound to $E_i^{\#}$ at a rate comparable to that in micelles. Significance of the exchange and equilibrium properties of the $E_i^{\#}$ complexes for the interpretation of the stationary phase reaction progress is discussed.
© 2005 Elsevier B.V. All rights reserved.

*Keywords:* Sphingomyelinase; *Bacillus cereus*; Interfacial catalytic turnover; Pseudo-scooting mode; Premicellar complex; Transferred NOESY

## 1. Introduction

SMase[1] (sphingomyelinase from *Bacillus cereus*) binds with high affinity to sphingomyelin (SM) vesicles, and the enzyme remains tightly bound to the vesicle interface during the highly processive interfacial catalytic turnover in the scooting mode [1]. Thus, during the steady-state in the scooting mode, the bound enzyme does not leave the interface. While the phosphocholine leaves the interface, the ceramide product remains in the target vesicle. At the end of the reaction progress, only the substrate on the external surface of the SMase-containing SM vesicles is hydrolyzed. Substrate present in the inner layer of the enzyme-containing vesicles, as well as in the excess vesicles to which the enzyme is not initially bound, is not hydrolyzed. In analogy with the behavior of secreted phospholipase $A_2$ such features of the reaction progress in the highly processive scooting mode show that the interface binding step is distinct from the catalytic turnover events [2–5], and that the catalytic site is different than the i-face (the interface binding surface) of the enzyme [6].

*Abbreviations:* $DC_7PC$, Diheptanoylphosphatidylcholine; HDNS, N-dansyl-hexadecyl-1-phosphoethanolamine; i-face, the interface binding surface of an interfacial enzyme; ITC, isothermal calorimetry; RET, fluorescence resonance energy transfer; SM, sphingomyelin; SMase, sphingomyelinase from *Bacillus cereus*; TMA-DPH, trimethylammonium-diphenylhexatriene

* Corresponding authors. Tel.: +1 302 831 2968; fax: +1 302 831 6335.
*E-mail address:* mkjain@udel.edu (M.K. Jain).

0005-2736/$ - see front matter © 2005 Elsevier B.V. All rights reserved.
doi:10.1016/j.bbamem.2005.03.009

Operationally, the i-face of an interfacial enzyme is designed to bind organized interfaces of amphiphiles. Therefore, it is not surprising that the i-face should also have a tendency to bind and organize monodisperse amphiphiles to form premicellar complexes as shown for phosphatidylinositol specific phospholipase C [7] and phospholipase $A_2$ [8,9]. Fig. 1 is a paradigm for this concept of premicellar $E_i^{\#}$ complex formation of interfacial enzymes with monodisperse amphiphiles (A), and also for understanding the relationship between the $E_i^{\#}$ complexes and the E* form at the preformed amphiphile interfaces (A*) such as micelles and bilayer vesicles. When A is SM, the concentration of monodisperse A will be very low not exceeding CMC ($<10^{-12}$ M). Under these conditions, both A and E will be more likely to go to the interface rather than forming $E_i^{\#}$; thus only E and E* will coexist in this case. However, if one component of a (mixed-)micellar dispersion is in significant monodisperse concentration, then E, $E_i^{\#}$ and E* can all coexist. On the other hand only E and $E_i^{\#}$ can coexist below the CMC with only the A form present.

In this paper, we analyze functional consequences of the coexistence of E, $E_i^{\#}$ and E* (Fig. 1) forms of SMase in the presence of $DC_7PC$. Not only is $DC_7PC$ bound to $E_i^{\#}$ in rapid exchange with the monodisperse amphiphile in the aqueous phase, but the $E_i^{\#}$ complex mediates a rapid exchange of SMase between the coexisting SM-containing interfaces which gives rise to the stationary phase in the reaction progress. Although the interfacial binding of the enzyme remains strong, the presence of monodisperse amphiphile and the concomitant formation of $E_i^{\#}$ complex allow rapid exchange of enzyme between micelles. As modeled in Appendix, the kinetic consequence is that the magnesium-dependent catalytic turnover by SMase occurs over an extended period of time without local depletion of the substrate on the enzyme-containing interface. Results are quantitatively interpreted with the assumption of ideal mixing of SM with the partitioned $DC_7PC$. Our analysis shows that not only do the $E_i^{\#}$ complexes mediate rapid exchange of the enzyme between the coexisting substrate-containing interface, but at >0.8 mole fraction $DC_7PC$ is also an ideal surface diluent for the SM interface. Our results show that the cooperative binding of monodisperse $DC_7PC$ molecules to the i-face of the enzyme sequentially forms the three premicellar complexes ($E_i^{\#}$). Since magnesium is required for the observed SMase-catalyzed hydrolysis [1,10,11], these results suggest an obligatory role for the cation in the binding of the enzyme to the interface. The dissociation constants for the bound $DC_7PC$ and the transferred NOESY results provide insights into the rapid exchange of A from $E_i^{\#}$ and micelles, presumably as multi-step fusion–fission kinetic process facilitated by step-wise removal of single amphiphile molecules.

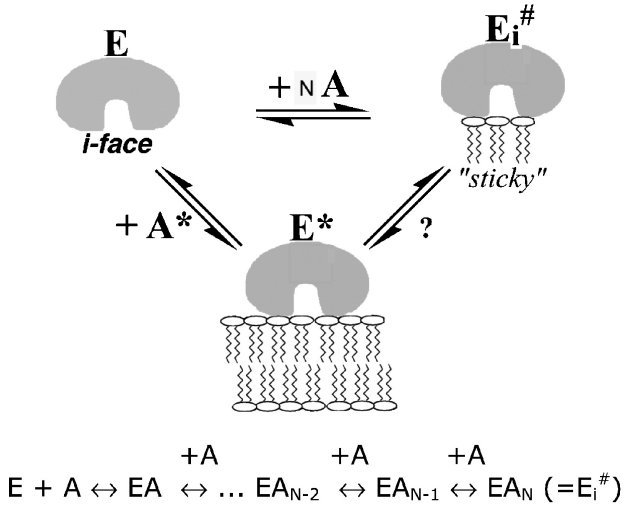


Fig. 1. A cartoon to conceptualize the cooperative binding of N monodisperse A ($DC_7PC$) or of aggregated A* amphiphiles to the i-face of SMase in the aqueous phase (E) to form $E_i^{\#}$ or E* complexes without the occupancy of the active site. Based on the evidence in this paper, $i=1, 2, 3$ for the three sequentially formed premicellar $E_i^{\#}$ complexes of SMase as shown by the fluorescence changes from the protein. On the other hand, as also shown in this paper, the amphiphile exchange rate monitored as NOESY signal is related to the association and dissociation of individual amphiphiles, i.e., $E_i^{\#}+A \leftrightarrow E_i^{\#}$ ($i=1, 2, 3$). In analogy to the micellization [4], this is one of the steps in the sequential equilibria as expanded in the lower part of the figure. Similar exchangeable discrete premicellar $E_i^{\#}$ that may represent the sub-states between E and E* are also formed with other interfacial enzymes [7–9] suggest that only certain discrete complexes.

## 2. Material and methods

### 2.1. Reagents

$DC_7PC$ was from Avanti. All other reagents were analytical grade. A preparation of SMase, expressed from the cloned SMase gene from *Bacillus cereus*, was purchased from Higata Shoyu Co. (Japan). It was further purified as described earlier [1], where we used the $OD_{280}$ of 23 for 1% SMase solution. Based on the W, Y and F content $OD_{280}$ is 16, and therefore based on this value, the turnover rates in this report are apparently 30% lower.

Unless mentioned otherwise, all measurements were carried out in 20 mM Tris buffer and 10 mM NaCl at pH 8 and 24 °C with indicated amount of added divalent cation. Stock solution of Tris and NaCl were filtered through a bed of Chelex to remove multivalent cations. The concentration of magnesium if present was kept at 3 mM that is at least 10 times above the apparent $K_d$ for magnesium for catalysis as well as for the binding of the $DC_7PC$ monomers. It is also sufficient to compete out trace amount of potent inhibitory cations in buffer. Control buffers in the absence of the divalent cation included 1 mM EDTA and 1 mM EGTA.

### 2.2. Kinetic measurements

Reaction progress for the hydrolysis of sonicated or extruded SM vesicles was monitored by pH-stat titration as

described before [1]. Reaction progress in 4 ml reaction mixture was continuously monitored at pH 8.0 and 24 °C in the nitrogen-purged environment by pH-stat titration with 1 mM amonipropanediol base calibrated with standard acetic acid. Other conditions are given in the legend to Figs. 2 and 4. Typically, the reaction was initiated by adding 0.5 to 10 μl volume of SMase to an otherwise complete assay mixture. Focus of this paper is on the stationary phase reaction progress observed in the presence of added $DC_7PC$.

### 2.3. Emission from intrinsic TRP fluorescence and the resonance energy transfer

These measurements were carried out on SLM-Aminco AB2 instrument set in the ratio mode at 4 nm slit widths for the emission and excitation wavelengths. In all measurements excitation was at 280 nm. Unless mentioned otherwise, the aqueous buffer contained 10 mM Tris and 20 mM NaCl at pH 8.0 in stirred cuvettes at 24 °C. Same conditions with excitation and emission at 360 nm were used for monitoring the decrease in the scattering of SM vesicles with added $DC_7PC$. For the energy transfer measurements, a constant ratio (given in the figure legends along with the emission wavelength) of the SMase donor and the probe acceptor was titrated with $DC_7PC$.

### 2.4. Isothermal calorimetric titration

ITC measurements were carried out on the Microcal calorimeter (model VP-itc) with cell volume of 1.42 ml with mechanical stirring at 300 rpm [7,8]. Standard software was used for the peak integration in relation to the internal calibration. The heat change associated with the dilution of monodisperse $DC_7PC$ per injection in the absence of the enzyme was negligible. The net heat change per injection of $DC_7PC$ in the presence of 5 μM SMase was integrated to obtain the total heat change as a function of the total added

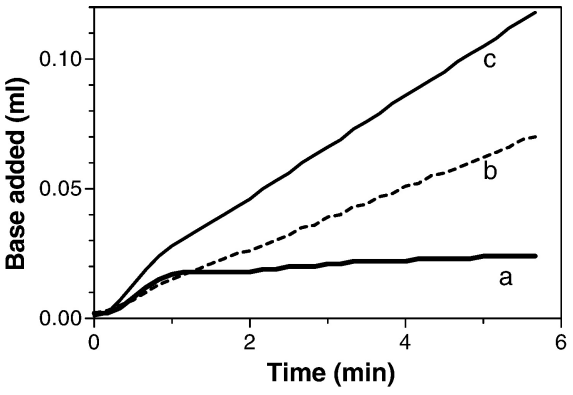


Fig. 2. Reaction progress curve for the SMase (9.6 pmol/4 ml reaction mixture at pH 8.0) catalyzed hydrolysis of the sonicated vesicles of sphingomyelin (0.2 mM; 800 nmol) (a) alone, or in the presence of (b) 1.3 mM and (c) 3.1 mM $DC_7PC$ at pH 8.0 in 10 mM NaCl and 3 mM $MgCl_2$. Calibration 1 ml base added = 1.6 μmol substrate hydrolyzed. Other conditions as described before [1].

$DC_7PC$ concentration in the cell. Although the formation of $E_1^{\#}$ complex was satisfactorily monitored by this method, titration at >0.4 mM $DC_7PC$ gave anomalous heat change that could not be satisfactorily resolved.

### 2.5. Anomalous retention of $E_i^{\#}$ on size-exclusion chromatography

The conditions and precautions necessary for the size-exclusion chromatography of the lipid–protein complexes of interfacial enzymes are described before [7–9]. Most of the size exclusion results in this paper were obtained on TSK-250 (250 × 7.5 mm) column from Bio-Rad, and some comparisons were also made with the Protein Pack 300 column (Waters). Elution was monitored on Rainin HPLC system equipped with sequential UV absorbance (at 280 nm) and fluorescence (excitation at 280 nm, emission at 340 nm) detectors with 15 μl flow cells. A comparison of the two outputs is useful to identify potential artifacts, such as the scattering contribution that interferes with estimation of the protein amounts from the peak area. The elution volume, $v_e$ for 34.5 kDa SMase was significantly larger than that expected from the calibration standards. Such secondary or anomalous retention, attributed to interaction with the column matrix [7,9,12], introduces considerable uncertainty in the size estimate.

### 2.6. NMR spectroscopy

Details of the transferred NOESY measurements are provided in the Supporting Information. For all NMR experiments, free $DC_7PC$ and $DC_7PC$+SMase samples were prepared in $^2H_2O$ with 3 mM added magnesium. The cation-free control measurements were made with 5 mM added $^2H$ labeled $D_{16}$-EDTA. Two-dimensional COSY, NOESY, ROESY and $^{13}C$-$^1H$ HSQC (natural abundance) spectra of 1 mM and 0.5 mM $DC_7PC$ solutions were obtained on a Bruker DRX-400 spectrometer operating at 400.13 MHz for protons, and 100.62 MHz for $^{13}C$ NOESY spectra were recorded with a mixing time of 350 ms. Transferred NOESY data for 1 mM $DC_7PC$ and 0.05 mM SMase complex in the absence and presence of 5 mM $D_{16}$-EDTA were recorded for mixing times: 10 ms, 20 ms, 50 ms, 80 ms, 100 ms, 120 ms, 150 ms, 200 ms, 250 ms, 300 ms and 350 ms. NOESY spectra with several mixing times (50 ms, 80 ms, 100 ms, 150 ms, 200 ms, 250 ms, 300 ms, 350 ms) were also recorded for $DC_7PC$ or $DC_8PC$ alone at 600 MHz on a Bruker Avance instrument. ROESY spectra were recorded for a mixing time of 60 ms with a spin-lock field of 4 kHz. TPPI scheme [13] was used for frequency discrimination in the indirect dimension in NOESY and ROESY spectra. NOESY and ROESY spectra were recorded as 300 × 2048 ((real) × (complex)) matrices with spectral widths of 2394.6 × 2394.6 Hz; COSY and HSQC spectra were acquired as 400 × 2048 ((real) × (complex)) matrices with spectral widths of (2394.6 × 2394.6) and

(10060.4 × 2394.6) Hz, respectively. COSY spectrum was recorded in a magnitude mode; TPPI scheme were used for frequency discrimination in the indirect dimension in the HSQC spectrum. Four transients were added in each $t_1$ increment; the recycle delays were 1.5 s. The data sets were processed using NMRPipe [14]. Resonance assignments and cross peak volume analysis was performed in Sparky [15]. Shifted sine bells were applied in both dimensions, and baseline correction was used in the directly detected dimension. For buildup rates, cross peak volumes were normalized to half of the sum of the corresponding diagonal peaks.

### 2.7. Simulations of transferred NOESY buildup curves

Simulations of the transferred NOESY buildup curves were performed as described previously [16] using a program written in Mathematica 5.0 (Wolfram Corp.) for each pair of protons in $DC_7PC$ assuming a single-step binding kinetics and using a 2-spin 4 × 4 relaxation-exchange matrix W. As detailed in the Supporting Information, the exchange rates for $DC_7PC$ bound to SMase or micelles complex were computed using the transferred NOESY buildup rates for the calibration pair of protons $H_1-H_2$ and assuming the minimal one-step binding model. The relaxation rates for the $DC_7PC$ bound to SMase were estimated assuming rotational correlation time of 16 ns (corresponding to the MW of SMase of 34.5 kDa).

## 3. Results

A major challenge for interfacial enzyme kinetic analysis is to be able to change the "interfacial concentration" (mole fraction) of the substrate and other active-site-directed ligands in the interface to which the enzyme is bound and remains bound during the steps of the turnover cycle [3,4]. In particular, for the interpretation of reaction progress in terms of a defined kinetic model by ensemble averaging, it is necessary to keep track of such changes during the reaction progress [4,17]. Also, surface dilution of the active-site-directed substrate and inhibitors in the interface requires a diluent amphiphile (A) that binds to the i-face of the enzyme but has no affinity for its active site [18]. If the codispersion of A with the substrate consists of small particles such as the mixed-micelles, the substrate replenishment rate on the enzyme-containing interface becomes rate-limiting rather than the interfacial turnover rate [4,19]. In Appendix, we use the detailed-balance condition for the coexistence of E, $E_i^{\#}$ and E* complexes (Fig. 1) of SMase with $DC_7PC$ and sphingomyelin to characterize the kinetic and biophysical consequences. Results show that under certain conditions, the interfacial turnover cycle remains rate limiting as the premicellar complex $E_i^{\#}$ of SMase with the surface diluent $DC_7PC$ rapidly exchanges between the substrate codispersions.

### 3.1. Stationary phase in the reaction progress in the presence of $C_7PC$ as a surface diluent for SMase

As shown in Fig. 2, the reaction progress in the highly processive scooting mode for the hydrolysis of sonicated SM vesicles in the absence of an additive reaches a maximum extent of hydrolysis even though more than 90% of the substrate remains unhydrolyzed. This is because the bound enzyme does not leave the vesicle to which it is initially bound and the substrate in excess vesicles without bound enzyme remains unhydrolyzed at the end of the reaction progress [1]. On the other hand, as also shown in Fig. 2, the reaction progress with a linear stationary phase continues in the presence of added $DC_7PC$ both below and above the CMC. Virtually, the same results were obtained with $DC_7PC$ added to large unilamellar vesicles (not shown).

Results in Fig. 3 show that the 90° scattered light intensity of SM vesicles decreases with added micellar $DC_7PC$, presumably because the SM vesicles are disrupted to form mixed-micelles. Note that the normalized scattering from the codispersions at excess $DC_7PC$ is virtually the same at 0.4 and 4 mM SM. However, the decrease in the scattering depends on the ratio of the two amphiphiles. Such a behavior cannot be adequately analyzed; however, the trend suggests nonideal mixing at >0.2 mole fraction SM based on the total concentrations present in the mixture. Based on this and additional evidence developed below and analyzed in terms of the model in Appendix, the $DC_7PC$-induced changes in the reaction progress are due to the exchange of SMase mediated by $E_i^{\#}$ complex (Fig. 1) between the SM-containing interfaces where the substrate is surface diluted by the partitioned $DC_7PC$. Two additional considerations are noteworthy.

(a) Formation of the premicellar complexes of SMase with SM or ceramide product is unlikely because the

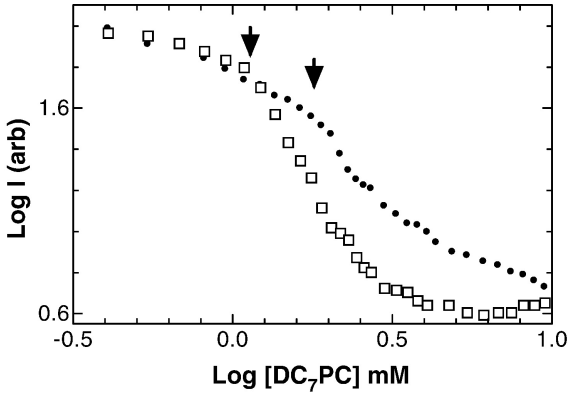


Fig. 3. Effect of added [$DC_7PC$] on the change in the normalized scattered light intensity (360 nm) of (square) 0.4 mM or (circle) 4 mM sphingomyelin vesicles (on the log–log scale) at pH 8.0 in 10 mM NaCl and 3 mM $MgCl_2$. The apparent shift in the CMC (marked with the arrows) is due to the depletion of $DC_7PC$ by partitioning into 4 mM SM. The titration curve at 4 mM SM also shows extended region of nonideal mixing.

expected CMC of SM and ceramide is $<10^{-12}$ M. Also even if such complexes could be present at subpicomolar concentrations, their contribution for the stationary phase reaction progress is unlikely to be noticeable because their exchange rate will also be exceedingly small. Moreover, tight binding of SMase and SM effectively precludes appearance of any premicellar complex under these conditions.

(b) As shown later, the exchange of $DC_7PC$ between the $E_i^{\#}$ complexes and micelles via the monodisperse $DC_7PC$ in the aqueous phase is rapid. Exchange rate for SM in vesicles through the aqueous phase between the codispersions is expected to be exceedingly small because the CMC is in the subpicomolar range. The SM replenishment by fusion and fission of the codispersions is also unlikely because the observed rate changes little with mixed-micelle concentrations at constant SM/$DC_7PC$ ratio (results not shown). The reaction progress in the enzyme-exchange mode [4,20] is fundamentally different from that of the quasi-scooting mode where a rapid substrate replenishment occurs either from the excess micelles via the monodisperse substrate in the aqueous phase [4,21] or through direct vesicle-to-vesicle exchange of the substrate [22,23]. In both of these cases, the turnover remains highly processive.

Results in Fig. 4 show the dependence of the observed initial rate of the SMase-catalyzed reaction on the mole fraction of SM. Biphasic behavior is seen with varying SM concentration at constant 6 mM or 3 mM $DC_7PC$. The fits shown in Fig. 4 are based on the model developed in Appendix where it is assumed that SM is ideally mixed with $DC_7PC$ as the surface diluent. They are also based on the equilibrium properties of the $E_i^{\#}$ complexes elucidated below. The fit is satisfactory below 0.25 mole fraction of SM. The best fit parameters for the results with 6 mM $DC_7PC$ can be used to predict the behavior also for 3 mM $DC_7PC$, at least in the major trends. The discrepancy in Fig. 4 could be explained by a very small shift in partitioning behavior; e.g., a decrease in $K_A'$ by ca. 3% would be sufficient to bring the predicted curve in accord with the experimental data. With $K_A' = 1.5$ mM (=CMC), the calculated interfacial turnover parameters are $k_{cat}^* = 350\ s^{-1}$ and $K_M^* = 0.12$ mole fraction. These values are in accord with $k_{cat}^* = 300\ s^{-1}$ and $K_M^* = 0.25$ mole fraction obtained by the dilution of SM from 1 to 0.7 mole fraction in bilayer of covesicles with 1-palmitoyl-2-oleoyl-phosphatidylcholine [1]. In these assays, the cation specificity for the turnover, as well as for the inhibition of the magnesium catalyzed reaction by the cations such as zinc and terbium, are in accord with those reported with other assays [10]. In these assays, inhibition was not observed with sphingocholine, alkylphosphocholine, or the noncompetitive inhibitor GW4869 [24]. This would be expected if these additives are not interfacial competitive inhibitors of SMase.

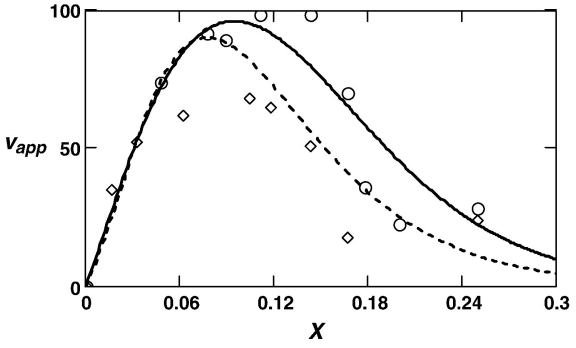


Fig. 4. The initial rate of the SMase-catalyzed hydrolysis of sphingomyelin codispersed in $DC_7PC$ at pH 8.0 in 10 mM NaCl and 3 mM $MgCl_2$ as dependent on the mole fraction $X$ of added SM. Results (circles) with 6 mM $DC_7PC$ and (diamonds) with 3 mM $DC_7PC$ and varying concentration of SM. The solid curve is the best fit from Eq. (A7) to the circles with $A_T = 6$ mM, giving the parameter set: $k_{cat}^* = 355\ s^{-1}$, $K_M^* = 0.12$ mole fraction, $K_A' = 1.5$ mM, $K_d = 8.9 \times 10^{-11}$ mM, and $k_{exch} = 12 * K_d^{eff}$. The dashed curve is expected enzyme rate from Eq. (A7) using the same parameter set and $A_T = 3$ mM.

Biophysical properties, including the equilibrium and exchange, of the $E_i^{\#}$ complexes of SMase are characterized below. Based on these results for the model in Appendix, we assume that the enzyme exchange between the substrate comicelles is mediated by the premicellar complex $E_i^{\#}$ of SMase with $DC_7PC$. This is a key assumption to account for the biphasic behavior in Fig. 4, that is the observed rate depends not only on the mole fraction of SM in the interface ($X_S^*$) and the amount of the bound enzyme but also on the rate of exchange of the bound enzyme mediated by $E_i^{\#}$ in the aqueous phase. The exchange parameters required for the fit shown in Fig. 4 are related to the exchange rate of SMase between SM+$DC_7PC$ codispersions. Based on the nonideality apparent in Fig. 3 at $X_S^* > 0.2$ we assume that SM is ideally mixed with $DC_7PC$ only at the lower mole fractions based on the total added concentrations. The micelle size assumed to be 200 is consistent with the interfacial turnover rate and the enzyme exchange rate.

Overall, the exchange rate for the fit in Fig. 4 is consistent with $K_d$ for the dissociation of E* to the E form as influenced by the formation of the $E_i^{\#}$ complexes. The rising parts of the curves in Fig. 4 are due to the increased availability of substrate in the interface. However, when the mole fraction of added SM is increased even further, most of it will form new interface that will draw more monodisperse $DC_7PC$ out of solution thereby decreasing the formation of $E_i^{\#}$ complexes (cf. Fig. A1 in Appendix). Thus, the falling parts are due to the slowdown in enzyme exchange rate when the concentration of free $DC_7PC$ decreases. Even though the concentration of monodisperse $DC_7PC$ is expected to be reduced only marginally, from 1.5 to ca. 1 mM at high $X_S^* = 0.3$ (with ideal partitioning), the exchange rate is very sensitive to this small change due to the high cooperativity of the $E_i^{\#}$-complex formation. As a consequence, the predicted enzyme rate in Fig. 4 is also extremely

sensitive to the partitioning behavior, to the micelle size, and to the value of $K'_A$.

### 3.2. Sequential formation of the premicellar $E_i^{\#}$ complexes of SMase

As shown in Fig. 5A, below the CMC=1.5 mM, the monodisperse-$DC_7PC$-dependent increase in the Trp fluorescence emission intensity of SMase depends on the presence of magnesium. In EDTA, virtually all the increase is seen above 1.1 mM $DC_7PC$ and it saturates above the CMC, and in the presence of magnesium virtually all the Trp-fluorescence increase occurs below the CMC. Our interpretation is that several $DC_7PC$ monomers cooperatively bind to SMase in the presence of magnesium. The fit shown in Fig. 5A is based on the following model [7,8]. The

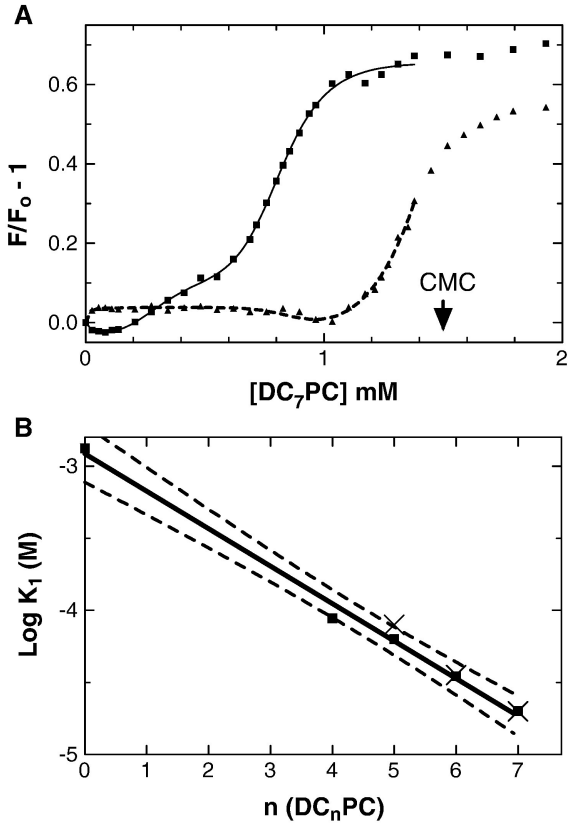


Fig. 5. (A) The effect of 3 mM magnesium (squares) or 1 mM EDTA+1 mM EGTA (triangles) on the Trp emission signal (excitation 280 nm, emission 340 nm) from 1 μM SMase in the presence of added DC7PC (CMC=1.5 mM). The increase in the emission intensity is also accompanied by a blue-shift. The smooth curves for the data points up to 1.35 mM were obtained with Eq. (2). The fit parameters in the presence of magnesium are $K_2$=0.33 mM and $K_3$=0.82 mM, with $a_i$ 0.14 and 0.66, and $n_i$=3.6 and 8.4. The parameter values for the first step were obtained from the itc measurements (Fig. 7). (B) Effect of the chain length on $K_1^{app}$, the apparent dissociation constant of $E_1^{\#}$ complex of SMase with diacylglycerophosphocholine, obtained from (squares) the Trp change or (crosses) the heat change (Table 1). The experimental point at the $y$-intercept is for the titration with glycerol-*sn*-3-phosphocholine ($n$=0). Dotted lines show the 95% confidence interval for the linear fit with slope −0.26 and $y$-intercept −2.85.

binding of monodisperse $DC_7PC$ to SMase can take place in at least three different ways. Based on the discernible steps in the presence of magnesium, we further assume that the complexes are formed sequentially as:

$$E \overset{n_1,K_1}{\leftrightarrows} E_1^{\#} \overset{n_2,K_2}{\leftrightarrows} E_2^{\#} \overset{n_3,K_3}{\leftrightarrows} E_3^{\#} \quad (1)$$

Each binding step is described by Hill parameter $n_i$ and dissociation constant $K_i$ ($i$=1, 2, 3). Assuming that the signal from the complex $E_1^{\#}$ is $a_1$, from $E_2^{\#}$ is $a_2$, and from $E_3^{\#}$ is $a_3$, the total signal can be expressed as:

$$S(E_T, A_f) = E_T \frac{(A_f/K_1)^{n_1}\{a_1 + (A_f/K_2)^{n_2}[a_2 + a_3(A_f/K_3)^{n_3}]\}}{1 + (A_f/K_1)^{n_1}\{a_1 + (A_f/K_2)^{n_2}[1 + (A_f/K_3)^{n_3}]\}} \quad (2)$$

where $E_T$ is the total concentration of enzyme and $A_f$ is the concentration of monodisperse $DC_7PC$. If the three binding steps are well separated, the nine parameters $n_1$, $n_2$, $n_3$, $K_1$, $K_2$, $K_3$, $a_1$, $a_2$ and $a_3$ can be estimated. If only two binding steps contribute, the result is given by Eq. (2) where all terms $(A_f/K_3)$ for the third step are set to zero. When the amphiphile concentration is in large excess over enzyme and therefore the $DC_7PC$ depletion is not significant [8], $A_f$ in Eq. (2) can be replaced by the total concentration $A_T$ of $DC_7PC$.

The fits shown in Fig. 5A are satisfactory for the cooperative three-step binding of monodisperse $DC_7PC$ to form three premicellar complexes in the presence of magnesium. The Trp signal for the first step is only about 3%. Therefore, reliable parameters for the magnesium-dependent formation of $E_1^{\#}$ were obtained also from the isothermal calorimetry results described below. The parameters for the second and third steps of the change in the Trp signal (Fig. 5A) clearly show that the magnesium-dependent formation of $E_2^{\#}$ and $E_3^{\#}$ are cooperative processes. Assuming that there is an all-or-nothing amphiphile binding, the Hill coefficients $n_i$ describe the apparent number of cooperative sites involved in the formation of the $E_i^{\#}$ complexes. Hill coefficient values $n_1$=3, $n_2$=3.6 and $n_3$=8.4 suggest that these complexes contain at least as many $DC_7PC$ molecules (=15) per SMase. The actual number of bound $DC_7PC$ per SMase would be higher if the amphiphiles were to bind with less than total cooperativity.

Formation of $E_1^{\#}$ with $DC_7PC$ is accompanied by a 3% fluorescence decrease (Fig. 5A). Small fluorescence changes were also observed with monodisperse $DC_6PC$, $DC_5PC$, $DC_4PC$ and glycerol-3-phosphocholine. $K_1^{app}$ values calculated from these changes are plotted in Fig. 5B as a function of the acyl chain length. As shown in this figure, comparable $K_1^{app}$ values were also obtained with isothermal calorimetric titration where Hill coefficients for the $E_1^{\#}$ complex with $DC_6PC$ and $DC_7PC$ were resolved (see below). The incremental $\delta\Delta G_{CH_2}^{app}$ of −0.35 kcal per methylene suggests that the hydrophobic contribution to the formation

of $E_1^{\#}$ is modest. On the other hand, the *y*-intercept is virtually the same with log $K_1^{app} = -2.85$ for glycerol-sn3-phosphocholine with no acyl chain, i.e., the free energy contribution for the interaction of glycerophosphocholine head group in the $E_1^{\#}$ complex is significant. The fit parameters for the formation of the $E_2^{\#}$ and $E_3^{\#}$ complexes with the shorter chain derivatives of phosphatidylcholines could not be adequately resolved because the stepwise fluorescence intensity changes were not adequately discernible.

The structure of SMase has not been determined. Its six Trp residues preclude structural assignments for the fluorescence changes. Also, we do not know if the stepwise changes in Fig. 5A are from the same or different Trp residues. Since $DC_7PC$ does not bind to the active site, the Trp signal is not attributed to the occupancy of the active site. Although the quenching results (not shown) for the $E_i^{\#}$ complexes could not be adequately resolved, they provide evidence for the clustering of $DC_7PC$ on the surface of SMase. Qualitatively, quenching of SMase by iodide, succinimide or acrylamide depends on the presence of magnesium as well as $DC_7PC$. Quenching of E and $E_1^{\#}$ is comparable, while less quenching is observed for the $E_2^{\#}$ and $E_3^{\#}$ complexes. This is expected if the quencher accessibility in the higher complexes decreases as the Trp residues are shielded due to the clustering of the bound amphiphiles as conceptualized in Fig. 1.

### 3.3. Isothermal calorimetric titration of SMase with $DC_7PC$

Suggestive evidence for the formation of $E_1^{\#}$ is provided by the results in Fig. 5A. As shown in Fig. 6, titration of 6 μM SMase with monodisperse $DC_7PC$ in the presence of magnesium induces an exothermic enthalpy change. The heat change is not observed in the absence of magnesium. The heat of dilution of the titrant in the absence of SMase was negligible in either of these buffers. Assuming depletion of three $DC_7PC$ bound to each SMase molecule, the fit for the heat change in the presence of magnesium was

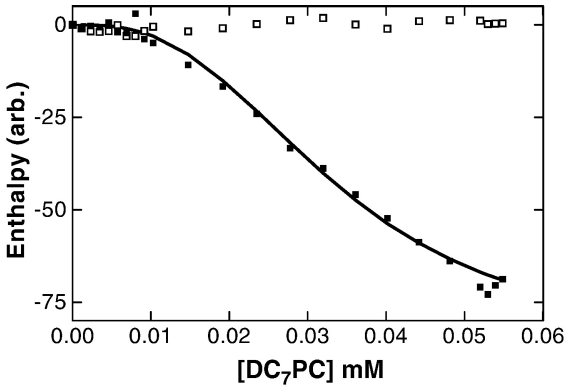


Fig. 6. Isothermal calorimetric titration of 6 μM SMase with 0.33 mM $DC_7PC$. Both solutions were prepared in 10 mM Tris at pH 8 and (filled square) 3 mM $MgCl_2$. Buffer for the magnesium-free run (unfilled square) contained 1 mM EGTA + 1 mM EDTA. The cell volume was 1.42 ml. The fit parameters for the itc titrations with $DC_nPC$ are summarized in Table 1.

obtained for a cooperative equilibrium binding of three monodisperse $DC_7PC$ with $K_1 = 0.02$ mM. The isothermal calorimetric fit parameters for the homologous $DC_nPC$ (Table 1) show that the first step for the binding of $DC_nPC$ in the presence of magnesium is exothermic. The value of the Hill coefficient $n_1$ for the hexanoyl and heptanoyl homologs is about 2. As compared in Fig. 5B, the calorimetric $K_1$ values are consistent with the $K_1^{app}$ values obtained from the Trp-fluorescence change. As summarized in table, the enthalpy change and the Hill number are lower for the lower homologs, which is consistent with the possibility that the hydrophobic effect of the alkyl chains stabilize $E_1^{\#}$. Together, the chain length dependence for the $DC_nPC$ binding suggests that the $E_1^{\#}$ formation involves not only the head group interactions, but also the hydrophobic effect presumably due to the desolvation of the i-face by the cluster of the acyl chains.

### 3.4. Partitioning of RET acceptor probes in $E_i^{\#}$

As conceptualized in Fig. 1, $DC_7PC$ molecules in $E_i^{\#}$ complexes are clustered on the i-face. Such a cluster would provide a distinct environment for the partitioning of a hydrophobic probe. As shown in Figs. 7 and 8, the energy transfer (RET) signal from a mixture of the SMase (donor) with TMA-DPH or HDNS acceptor changes as different $E_i^{\#}$ are formed. Thus, the change in the signal with added monodisperse $DC_7PC$ is from a difference in the extents to which the donor and acceptor are colocalized in the $E_i^{\#}$ complex formed under those conditions. In both cases, the signal is seen only in the presence of magnesium suggesting that magnesium is required for the clustering of $DC_7PC$ in the $E_i^{\#}$ complexes. Controls also show that the change in the probe with added $DC_7PC$ is insignificant in the monomer range and is modest in the micellar range.

As expected the change in the signal from the SMase + probe mixture as a function of $DC_7PC$ concentration is multiphasic. Although the steps are not well resolved, in both cases the RET signal from $E_3^{\#}$ is larger than that from $E_2^{\#}$. As expected, near and above the CMC, the signal decreases as the partitioned probe is diluted into the excess $DC_7PC$ micelles. In addition, results in Fig. 7 show that magnesium is not required for the binding of SMase to micellar $DC_7PC$. Also, the RET signal from TMA-DPH partitioned into dimyristoylphosphatidylcholine (DMPC) vesicles in the presence of SMase is observed with or without magnesium (results not shown). It is, however, intriguing that the binding of SMase to DMPC vesicles containing HDNS (see below) did not give the RET signal.

The RET signal from HDNS (Fig. 8) as a function of $DC_7PC$ added to SMase is multiphasic, and a large increase corresponds to the formation of $E_2^{\#}$ and $E_3^{\#}$. A parallel decrease in the emission from Trp donor (not shown) provided evidence for the resonance energy transfer. These results show that the $E_2^{\#}$ and $E_3^{\#}$ complexes offer a favorable environment for the colocalization of SMase with HDNS.

Table 1
Fit parameters[a] for the isothermal calorimetric titration of SMase with homologous $DC_nPC$

| $n$ | $K_1$ (mM) | $n_1$ | Enthalpy (kcal/mol) |
|---|---|---|---|
| 7 | 0.025 | 3 | −7.1 |
| 6 | 0.036 | 2 | −1.8 |
| 5 | 0.08 | 2 | −0.5 |

[a] Uncertainty in the parameter values is estimated to be 30%.

At the higher $DC_7PC$ concentrations near the CMC the RET signal reaches the background level seen with SMase in the presence of EDTA. Together, the probe partitioning behavior, monitored as the RET signal in Figs. 7 and 8, shows that in the presence of magnesium $DC_7PC$ molecules are clustered in the premicellar $E_2^{\#}$ and $E_3^{\#}$ complexes. As discussed elsewhere [7], for a variety of reasons, it is not possible to quantitatively interpret such RET results in terms of the primary equilibrium events.

### 3.5. Anomalous size-exclusion of $E_i^{\#}$

Results in Fig. 9 show that $E_i^{\#}$ complexes of SMase exhibit anomalous interaction with the size-exclusion matrix. The E* form of SMase elutes as a 55-kDa complex in micellar 3 mM $DC_7PC$ and magnesium, and a somewhat smaller complex is formed in EDTA. As is the case with the results in Figs. 7 and 8, it is not possible to quantitatively interpret the anomalous retention results. However, these results are consistent with the suggestion that the cluster of the bound $DC_7PC$ molecules on $E_i^{\#}$ provides an exposed hydrophobic surface as conceptualized in Fig. 1. In accord with our earlier results [12], we attribute the anomalous retention to the interactions of $E_i^{\#}$ complexes with the exposed hydrophobic patches on the column matrix. Note that SMase is anomalously retained in the presence of monodisperse $DC_7PC$ in the elution buffer in the presence of EDTA. This is consistent with the NOESY results described below, and with the suggested Mg-induced activation.

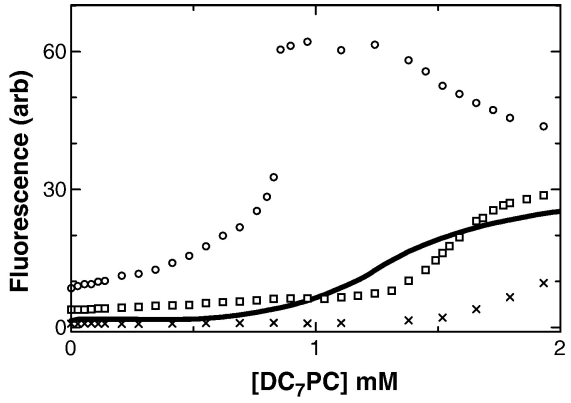


Fig. 7. $DC_7PC$ concentration-dependent change in the RET signal (em 450 nm, ex 280 nm) from 1 μM TMA-DPH in the presence of (cross) no SMase, or in the presence of 0.9 μM SMase in the buffer containing (squares) 1 mM EDTA or (circles) 3 mM Mg. The continuous line shows the change in the normalized Trp emission intensity at 340 nm from SMase in the presence of EDTA (from Fig. 5A). Note that the change in the RET signal from the probe is steeper than in the Trp signal. The emission signal from the cationic TMA-DPH increases when it is partitioned in micelles, and an additional increase from the RET signal is seen when the probe is colocalized with SMase in $E_i^{\#}$. Also, the change in the initial emission from the probe is modestly different in the presence of SMase and magnesium.

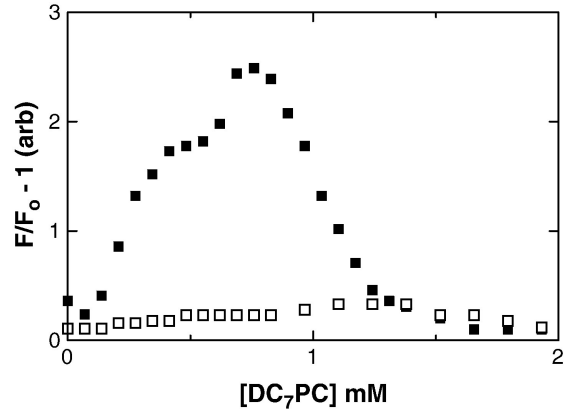


Fig. 8. The change in the RET signal with $DC_7PC$ concentration in a mixture of 0.5 μM SMase, 1 μM HDNS (CMC = 10 μM), and (unfilled squares) 1 mM EDTA + 1 mM EGTA, or (filled squares) in 10 mM $MgCl_2$. The reaction mixture contained 10 mM Tris, 1 mM NaCl at pH 8 and 24°C.

### 3.6. Effective NOESY buildup rates of $DC_7PC$ free and complexed with SMase

Assignments of $^1H$ and $^{13}C$ resonances in $DC_7PC$ shown in Fig. 10 are based on a combination of COSY and $^{13}C$-$^1H$ HSQC spectra of 1 mM $DC_7PC$ (see Supporting Information). For the analysis of $DC_7PC$ binding to SMase, we focused on the calibration pair of protons $H^1-H^2$ with fixed distance. We solely refer to this pair for the interpretation of the transferred NOESY data because the NOESY enhancement is due to the binding without a contribution from the

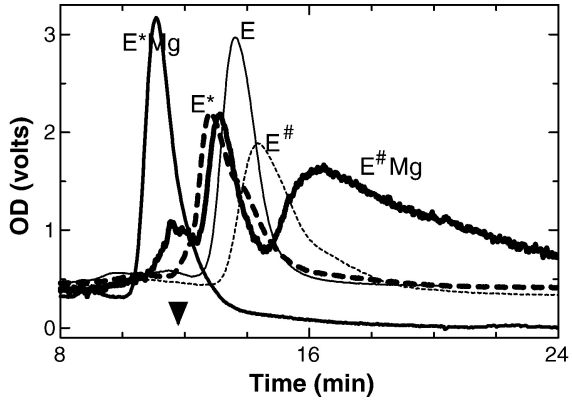


Fig. 9. The elution profiles in the presence of 10 mM $MgCl_2$ for SMase alone (thin continuous line, E), or with 3 mM $DC_7PC$ (medium continuous line, E*Mg) or 0.7 mM $DC_7PC$ (thick continuous line, $E^{\#}Mg$). The dashed lines show the elution profiles for SMase in 3 mM (E*) or 0.7 mM ($E^{\#}$) $DC_7PC$ in the presence of 1 mM EDTA in the buffer. The ordinate for $E^{\#}Mg$ is expanded by a factor of six. Flow rate 1 ml/min. Void volume 4.6 ml. Comparable results were obtained on the Pharmacia Bio-Sil and TSK-250 columns. Note that SMase is anomalously retained. Expected elution time for SMase alone is marked on the $x$-axis.

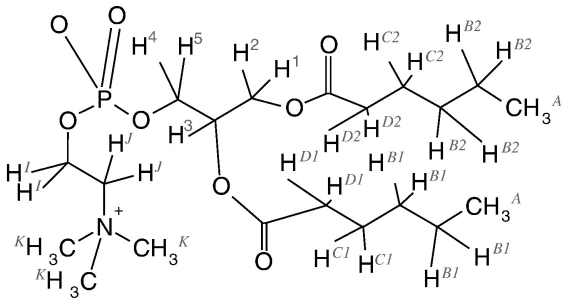

Fig. 10. $DC_7PC$ structure with hydrogen labels.

conformational change. Detailed expressions for calculations of the transferred NOESY buildup rates have been derived previously and are presented in the Supporting Information. Below, we discuss the salient contributions to the transferred NOE cross peaks and buildup rates.

In the limit of fast exchange, short mixing times and assuming one-step binding [25], the transferred NOESY cross-relaxation rates are linear functions of the mixing time, and for each pair of interacting protons can be expressed as the population-weighted averages of the cross-relaxation rates corresponding to the free and the bound forms:

$$a_{ij}(\tau_m) \cong -\left[p_{\mathcal{B}}\sigma_{ij}^{\mathcal{B}} + p_{\mathcal{F}}\sigma_{ij}^{\mathcal{F}}\right]\tau_m \qquad (3)$$

where $\sigma_{ij}^{\mathcal{B}}$ and $\sigma_{ij}^{\mathcal{F}}$ are the cross-relaxation rate constants of the bound and free ligand (Eq. (4)), experimentally related to the cross-peak volumes. $p_{\mathcal{B}}$ and $p_{\mathcal{F}}$ are the fractions of the bound and free ligand, in the limit of diffusion-limited one-step binding determined by the concentration of the interacting species and the equilibrium dissociation constant.

The cross-relaxation rate constants between spins $i$ and $j$ are functions of the effective molecular weight, proton–proton distances and magnetic field strength:

$$\sigma_{ij} = \frac{\hbar^2\gamma_{\mathcal{H}}^2}{10}\left(\frac{\mu_0}{4\pi}\right)\frac{1}{r_{ij}^6}\left(-\tau_c + \frac{6\tau_c}{1+(2\omega_{\mathcal{H}}\tau_c)^2}\right) \qquad (4)$$

where $\gamma_{\mathcal{H}}$ is the proton gyromagnetic ratio; $r_{ij}$ is the interproton distance; $\omega_{\mathcal{H}}$ is the proton Larmor frequency; $\hbar$ the reduced Planck's constant; $\mu_0$ is the magnetic permeability of vacuum. $\tau_c$ is the isotropic rotational correlation time and is estimated from the Stokes' law: $\tau_c = \frac{4\pi\eta_w r_{\mathcal{H}}^3}{3k_{\mathcal{B}}\mathcal{T}}$. $\eta_w$ is the viscosity of the solvent; $r_{\mathcal{H}}$ is the effective hydrodynamic radius of the protein, $k_{\mathcal{B}}$ is the Boltzmann's constant, and $\mathcal{T}$ is the temperature. For isotropic proteins, $\tau_c$ is approximately linear with the molecular weight and is ca. 0.4 ns per 1 kDa. For a pair of protons with known distance, these cross-relaxation rates can be readily calculated.

Therefore, the effective transferred NOESY buildup rates for calibration protons in $DC_7PC$/SMase relate to the residence time of $DC_7PC$ on the complex and the effective size of the complex. As shown in Fig. 11, strong transferred NOESY enhancement observed with SMase in 1 mM $DC_7PC$ is presumably from a mixture of the $E_2^{\#}$ and $E_3^{\#}$ complexes. As expected, the diagonal and cross peaks are exchange-broadened in the complex. The relative normalized volumes of all cross peaks in the spectra of the complex are somewhat stronger than in the micellar $DC_7PC$ but somewhat weaker than in the micellar $DC_8PC$. It permits an estimate of the monomer exchange time and therefore an estimate of the amphiphile monomer binding constant to the complex. Note that the effective dissociation constant

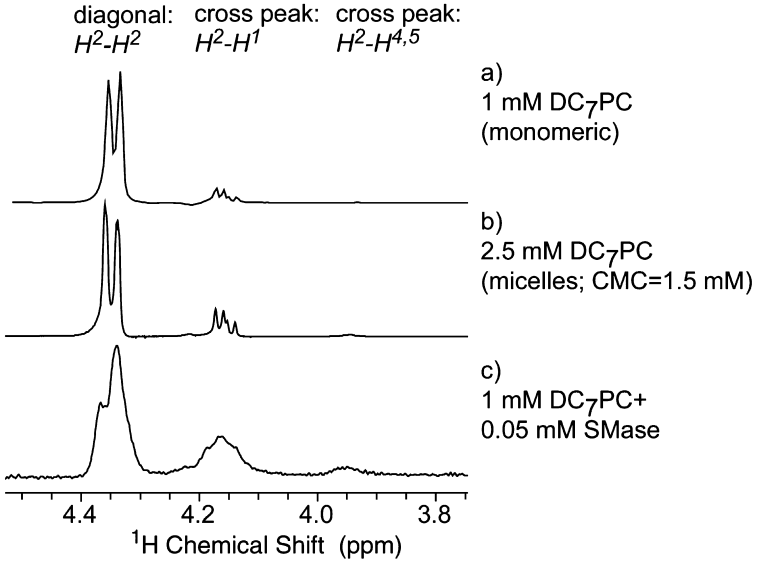


Fig. 11. $t_2$ projections of the NOESY spectra ($\tau_{mix}$=250 ms) illustrating the relative cross peak intensities (from top) for the calibration pair of protons $H^1$ and $H^2$ in (a) 1 mM predominantly monomeric $DC_7PC$; (b) 2.5 mM micellar $DC_7PC$; (c) 1 mM DC7PC/0.05 mM SMase complex. Strong positive cross peaks (ca. 32–53% of the diagonal peak volumes at this mixing time) for 1 mM $DC_7PC$ bound to SMase are due to the transferred NOESY enhancement. Weak transferred NOESY enhancement is also observed for the 2.5 mM micellar $DC_7PC$.

obtained from the exchange kinetics is comparable to $K_3$ for $E_3^{\#}$ or the CMC. Also, in conjunction with other results discussed below, we suggest that the transferred NOESY results relate to the exchange kinetics for the monomer amphiphile bound to $E_3^{\#}$ or micelles.

With the aggregation number of 70, the effective MW of a $DC_7PC$ micelle would be about 34 kDa. Similarly, with about 15 $DC_7PC$ bound to an SMase the MW of $E_3^{\#}$ complex would be about 40 kDa, which alone would give a very modest increase in the $I_{cross}/I_{diag}$ ratio (assuming similar equilibrium dissociation constants), undetectable within the experimental error. Therefore, the larger buildup rate in the 1 mM $DC_7PC$/0.05 mM SMase complex (Table 2) indicates a somewhat larger relative population of the bound species at these concentrations. If the on-rate is diffusion limited, the observed differences in the transferred NOESY enhancement for the same size aggregates can be attributed to the differences in the relative populations of the free and the bound species, determined by the monomer dissociation constant. These results qualitatively suggest that the effective monomer/amphiphile exchange rate for the $E_3^{\#}$ complex is somewhat larger than in $DC_7PC$ micelles. On the other hand, the buildup rates in the 1 mM $DC_7PC$/0.05 mM SMase complex are weaker than those observed in the micelles of $DC_8PC$ with MW of about 65 kDa for an aggregation number of 120. Even though the different sizes of the aggregates for micellar $DC_8PC$ and $DC_7PC$/SMase complex do not allow for a direct comparison of the buildup rates, qualitatively the results indicate that the effective population of the bound species in the 1 mM $DC_7PC$/0.05 mM SMase complex is comparable with the micellar $DC_8PC$, but could be either slightly higher or slightly lower. The rates for 1 mM $DC_7PC$/0.1 mM SMase (Table 2) show that, as expected, the increased protein concentration results in stronger transferred NOESY enhancement due to the increased population of the bound species.

## 4. Discussion

The natural substrate for bacterial SMase, a toxin for animal cells, is sphingomyelin codispersed with phosphatidylcholine in eukaryotic plasma membrane [26,27]. The magnesium-dependent neutral SMase in human cells is likely to have a similar substrate interface [28,29], although its function is not known. Our results show that SMase binds not only to phosphatidylcholine vesicles [1] but monodispersed phosphatidylcholines such as $DC_7PC$ also cooperatively bind to the interface-binding surface (not to the active site) of SMase in a range of their submicellar concentrations only in the presence of $Mg^{2+}$. The kinetics of SMase-catalyzed hydrolysis of SM dispersed in $DC_7PC$ micelles showed that the turnover in the stationary phase is due to the exchange of the SMase mediated through the premicellar complexes with $DC_7PC$ ($E_i^{\#}$). The proposed method for analysis and the obtained result are of general interest for evaluating the significance of assays with mixed-micellar substrate.

The structural basis and the mechanism for the magnesium requirement for the SMase activity [30], including the processive turnover [1], is not established. The $Mg^{2+}$ requirement for the formation of the premicellar complexes of SMase with the monodisperse $DC_7PC$ is of particular interest. The magnesium concentration dependence of the observed rate depends on the nature of the interface, which suggests a role for magnesium in the interface binding and possibly also in the events of the interfacial turnover cycle. Both of these processes are saturated at 3 mM $Mg^{2+}$ used in this study. A key result in this paper is that magnesium is obligatorily required for the cooperative binding of several $DC_7PC$ monomers to SMase without the catalytic turnover or the occupancy of the active site. Since the interface binding step obligatorily precedes the interfacial turnover, we suggest that a role for magnesium in the cooperative binding of $DC_7PC$ to the i-face of SMase is related to the allosteric activation which promotes the binding of SMase to the interface in a catalytically competent form. It is, however, intriguing that SMase also binds to zwitterionic interface even in the absence of the cation, which suggests that this form of the enzyme is not allosterically activated. Characterization of $E_i^{\#}$ species and the conditions for its crystallization can provide information about the i-face in the interfacially activated form of SMase. The monomer exchange rate is for the rapidly exchanging amphiphiles in $E_i^{\#}$, and such a process could contribute multiple sequential steps to facilitate the exchange of $E_i^{\#}$ between the coexisting interfaces.

Table 2
Effective NOESY buildup rates[a] for $DC_7PC$ (+A) free and complexed with SMase (+E)

| Sample | Effective NOESY buildup rate, $s^{-1}$ | Aggregation number | $MW_{eff}$, g/mol | $\tau_c$, ns | Cross-relaxation rate, $s^{-1}$ |
|---|---|---|---|---|---|
| 1 mM A | 0.7±0.2 | 1 | 481.56 | 0.3 | 0.33 |
| 1 mM A+0.05 mM E | 0.9±0.2 | 15 A+1 E | 40,000 | 16 | −48[b] |
| 1 mM A+0.1 mM E | 1.7±0.2 | 15 A+1 E | 40,000 | 16 | −48[b] |
| 2.5 mM A | 0.8±0.2 | ~70 | ~34,000 | 14 | −42[b] |
| 0.11 mM $DC_8PC$ | −0.8±0.2 | 1 | 509.62 | 0.2 | 0.22 |
| 1.1 mM $DC_8PC$ | 1.1±0.2 | ~120 | ~65,000 | 26 | −78[b] |

[a] Effective rates were estimated as linear slopes of the corresponding buildup curves for the calibration pair of protons.
[b] Cross-relaxation rate of the bound form is given. The cross-relaxation rate of the free species is given in the corresponding entry for the monomeric amphiphile.

### 4.1. $E_i^{\#}$-exchange-mediated stationary phase reaction progress

$DC_7PC$ is neither a substrate nor an active-site-directed ligand for SMase. On the other hand, as a basis for the turnover in the stationary phase, $E_i^{\#}$ complex of $DC_7PC$ mediate the exchange of SMase between the coexisting substrate interface of the codispersions of SM + $DC_7PC$. This model adequately accounts for the observed characteristics of the reaction progress in the presence of $DC_7PC$. The observed rate depends on the stability of the $E_i^{\#}$ and E* complexes as well as the concentration and relative mole fraction of the substrate and diluent. Within the assumption of ideal mixing of SM and $DC_7PC$, the predictions of the model provide an adequate description of the observed kinetic behaviors (Figs. 2 and 4). For example up to 0.1 mole fraction SM, the $E^* \leftrightarrow E_i^{\#}$ exchange rate, and therefore the residence time of the enzyme on the interface, is adequate to give a stationary rate that remains limited by the steps of the interfacial turnover path. This is the $E_i^{\#}$-exchange-mediated stationary reaction progress. With larger amounts of SM, the concentration of monodisperse $DC_7PC$ decreases, less $E_i^{\#}$ is formed and enzyme exchange becomes limiting. Thus, the biphasic dependence of the observed linear stationary rates on the $X_S$* is accounted for by the assumption of ideal partitioning and mixing of $DC_7PC$ with SM [4]. However, departure from the ideal behavior is expected and is clearly apparent in the results in Fig. 4. The outcome of such second-order effects and non-idealities remains to be analyzed.

### 4.2. Contributions to the $E^* \leftrightarrow E_i^{\#}$ exchange

Over the decades, we have developed [3–5,7,8] ways to dissect and model the interfacial kinetic behaviors in terms of the interfacial turnover cycle. Our strategy is to evaluate the primary rate and equilibrium parameters for the i-face and active site interactions in the context of $k_{cat}$* for the rate limiting chemical step in an unequivocally defined turnover path. Our present results provide a unique window of conditions for the rapid exchange of the enzyme between the coexisting interface where the interfacial turnover steps remain rate limiting. The minimum model to evaluate the contribution of the $E^* \leftrightarrow E_i^{\#}$ exchange during the stationary phase of the reaction progress is outlined in Fig. 1, and the parameters for the action of SMase on SM + $DC_7PC$ codispersions are independently determined. E* and $E_i^{\#}$ complexes of SMase are formed in the presence of magnesium, and the dissociation constants for the three $E_i^{\#}$ complexes with $DC_7PC$ are $K_1 = 0.025$, $K_2 = 0.2$ and $K_3 = 0.8$ mM. The Trp signal for the formation of $E_1^{\#}$ is weak (Fig. 5A). On the other hand, the heat change is significant only for the formation of $E_1^{\#}$ in the presence of magnesium, which may be associated with a conformational change in SMase as precursor to the cooperative binding of additional $DC_7PC$ molecules to the i-face of SMase. At this stage, we do not know how such a change is translated into an allosteric effect on the interfacial turnover events.

Although the active E* complex is formed with high affinity, it is effectively destabilized by the presence of the premicellar $E_i^{\#}$-complexes. This has two counteracting effects on the overall enzyme kinetics: the reduction in the amount of active E* reduces the turnover rate at the same time as the $E_i^{\#}$-mediated enzyme exchange increases turnover. The effects are very sensitive to the details of the partitioning and interfacial mixing due to the cooperative nature of the premicellar complex formation. Thus, the kinetic behavior of the enzyme can be strongly influenced by relatively small changes in monodisperse amphiphile concentrations.

### 4.3. Limitations of the turnover path during the stationary-state rate

We have established conditions for the reaction progress in the scooting mode where the steady state behavior is described by summation of the events of the interfacial turnover cycle [1,4,17,21]. This critical condition for ensemble averaging is met for a modified turnover path and with certain additional assumptions. The initial rate can be defined from the stationary state with linear reaction progress that appears before substrate has been depleted. The interfacial enzymes "see" only the interfacial substrate concentration, $X_S$*, and a true initial rate would require that this local concentration has not been depleted. There are a number of situations where this initial rate could be observed also for the interfacial enzymes: with very large aggregates where the local $X_S$* will decrease only slowly, with fast replenishment of substrate from solution or other aggregates, or with fast enzyme exchange so that each enzyme moves to a fresh aggregate before a significant reduction of $X_S$* has occurred. This latter situation is at hand in this study at low SM addition when a high concentration of monodisperse $DC_7PC$ allows a fast $E_i^{\#}$-assisted exchange. If exchange is slow, each aggregate will be significantly depleted before the enzyme moves on to a fresh aggregate and starts depletion anew. As long as there are fresh untouched aggregates present (low enzyme-to-aggregate ratio), there will be an exchange-limited stationary state determined effectively by the exchange rate and the number of substrates hydrolyzed in each visit. This is the apparent initial rate plotted in Fig. 4 at high SM addition where the lower monodisperse $DC_7PC$ concentration slows down the $E_i^{\#}$-assisted exchange.

Considering the complexities involved in the origins of the stationary phase reaction progress, we believe that such assay systems cannot be used to obtain information about the primary interfacial turnover events. This is amply demonstrated by the fact that assays with detergent dispersed substrates which give apparently linear initial rates have not been useful for the characterization of the

effects of the kinetic variables including the characterization of the site-directed mutants [3,19].

### 4.4. Exchange kinetics of $DC_7PC$ bound to $E_3^{\#}$ of SMase

The exchange kinetics of $DC_7PC$ bound to $E_3^{\#}$ complex of SMase is qualitatively comparable to that of $DC_7PC$ and $DC_8PC$ exchange in micelles (Table 2). The NOESY buildup rate in the 1 mM $DC_7PC$/0.05 mM SMase complex is somewhat larger than in the 2.5 mM micellar $DC_7PC$. The exchange rate for the micellization process is ca. $1.5 \times 10^6$ $s^{-1}$ estimated from the critical micelle concentration of 1.5 mM [31,32] and the diffusion limited rate constant $k_{on}$ of $10^9$ $M/s^{-1}$. Since the size of the $DC_7PC$ micellar aggregates at 2.5 mM is similar to the size of $DC_7PC$/SMase complex, and both types of species are globular, we conclude that the equilibrium exchange between monomeric solution and protein interface-bound forms of amphiphile is likely to take place at rates slightly slower than $1.5 \times 10^6$ $s^{-1}$. This conclusion is consistent with the numerical simulations of the buildup rates at both protein to amphiphile ratios (Fig. 12), indicating good agreement with experimental results for exchange rates between 0.3 and $1.5 \times 10^6$ $s^{-1}$.

## 5. Conclusion

Results in this paper mark a milestone for the analysis of interfacial enzyme. It is very likely that the premicellar $E_i^{\#}$ complexes are the sub-states formed in the E to E* step. If so, these complexes offer an opportunity to study the structural and functional changes associated with the activation of the enzyme by the amphiphile interactions along the i-face. The main focus of this paper is on the kinetic results that show that the $E_i^{\#}$ complexes are well suited for mediating the exchange of the enzyme in the codispersions of SM with $DC_7PC$. An apparent kinetic advantage of the $E_i^{\#}$-mediated exchange is that it circumvents problems associated with direct E ↔ E* exchange that may be slower on the time scale of catalytic turnover cycle. However, such a stationary phase casts serious doubts about the efficacy of the assays with mixed-micelles for the interpretation of kinetic mechanism [33,34]. Our results clearly show that the extended stationary phase reaction progress cannot be interpreted as the steady state. Such concerns apply to virtually all the anomalous kinetic effects of temperature or product-accumulation on the bilayer phase properties [4]. In all such cases, our experience is that the major effect of the 'quality of interface' is on the variables for the interfacial turnover and processivity.

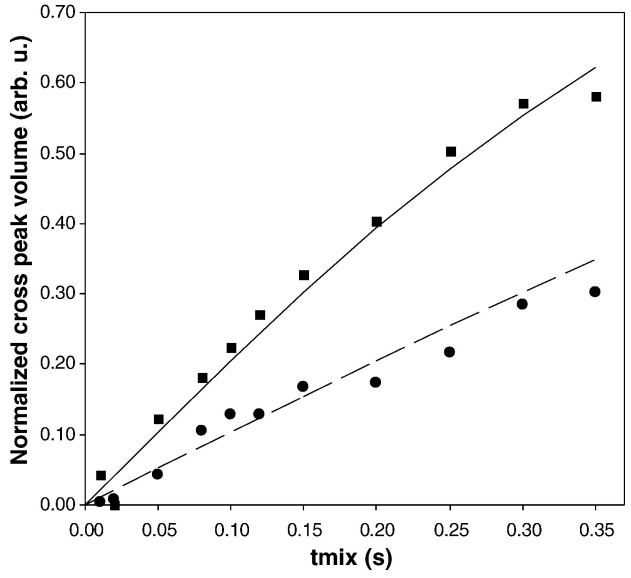


Fig. 12. Experimental and simulated transferred NOESY buildup curves for a calibration pair of protons $H^1-H^2$ in (a) 1 mM $DC_7PC$/0.05 mM SMase (filled circles); (b) 1 mM $DC_7PC$/0.1 mM SMase (filled squares, top). The solid and dashed lines represent best fits to the data, assuming non-cooperative one-step binding with $K_d$=1.5 mM. The cross peak volumes were normalized with respect to one half of the sum of the corresponding diagonal peaks.

## Acknowledgements

This research was funded by PHS (GM29703 to MKJ), NSF-CAREER (CHE-0350385 to TP), NIH-Cobre (P20-17716 to TP) and Swedish Research Council (to OGB). TP also acknowledges INBRE program of NCRR (RR016472-04 and purchase of the solution NMR instrument).

## Appendix A. Ideal partitioning of SM into mixed micelles with $DC_7PC$

Consider a mixture of SM (=$S$) at total concentration $S_T$ with $DC_7PC$ (=$A$) at total concentration $A_T$. $DC_7PC$ above its CMC (=$K'_A$ =1.5 mM) is present as micelles (A*); all the added SM mixes and partitions into the A* micelles; SM has very low CMC ($K'_S \ll K'_A$) and there will be (almost) no free $S$ in solution. The presence of S, at mole fraction $X_S$*, in the micelles will allow more $A$ to partition. The assumption for ideal mixing in the interface is that the partitioning of $A$ depends only on the amount and not the composition of the interface so that the concentration ($A_f$=IMC) of free $A$ in solution is determined by:

$$A_f = K'_A(1 - X_S^*) \tag{A1}$$

Furthermore, the total concentration of interface will be

$$M^* = S_T + A_T - A_f = A_T/(1 - X_S^*) - K'_A \tag{A2}$$

With these assumptions, the mole fraction of S in the micelles will be:

$$X_S^* = \frac{A_T + S_T - K'_A}{2K'_A}\left\{\pm\sqrt{1 + \frac{4S_TK'_A}{(A_T + S_T - K'_A)^2}} - 1\right\} \tag{A3}$$

(The + sign is when $A_T+S_T>K'_A$, otherwise −). At constant $A_T=6$ mM, $X_S$* and $A_f$ will change with the added mole fraction of S, $X=S_T/(S_T+A_T)$, as shown in Fig. A1. Based on the results at hand, it appears that the ideal partitioning behavior may be a reasonable approximation up to about $X_S$*=0.3 mole fraction SM in $DC_7PC$.

## Appendix B. Distribution of enzyme

Based on the evidence in this paper we assume that SMase (=E) can interact with the amphiphiles in a number of ways:

$$E_3^{\#} \overset{n_3,K_1}{\rightleftharpoons} E_2^{\#} \overset{n_2,K_2}{\rightleftharpoons} E_1^{\#} \overset{n_1,K_3}{\rightleftharpoons} E \underset{K_d}{\rightleftharpoons} E^* \underset{K_M^*}{\rightleftharpoons} E^*S \xrightarrow{k_{cat}^*} \quad \text{(A4)}$$

The premicellar states ($E_i^{\#}$) are complexes with monodisperse A in solution that will effectively destabilize the active enzyme bound at the interface, E*. As a consequence, the effective dissociation constant for E* to any of the solution species, E or $E_i^{\#}$, can be expressed as

$$K_d^{eff} = K_d\left\{1+\left(\frac{A_f}{K_1}\right)^{n_1}\left[1+\left(\frac{A_f}{K_2}\right)^{n_2}\left(1+\left(\frac{A_f}{K_3}\right)^{n_3}\right)\right]\right\} \quad \text{(A5)}$$

where $K_d$ is the dissociation constant if no premicellar complexes can form. Although, the concentration ($A_f$) of free A varies relatively little with changing amounts of S (Fig. A1), the change in $K_d^{eff}$ is over several orders of magnitude (Fig. A2, note the logarithmic scale) due to the cooperative nature of the premicellar complex formation.

As only E* is active, the initial rate for the enzyme in this scheme will be

$$v_i = \frac{k_{cat}^* X_S^*}{K_M^* + K_M^*\left(K_d^{eff}/M^*\right) + X_S^*} \quad \text{(A6)}$$

This initial rate would be observable for an extended period of time if exchange is sufficiently fast, i.e., if the enzyme exchanges sufficiently fast between micelles so that substrate is not significantly depleted in enzyme-

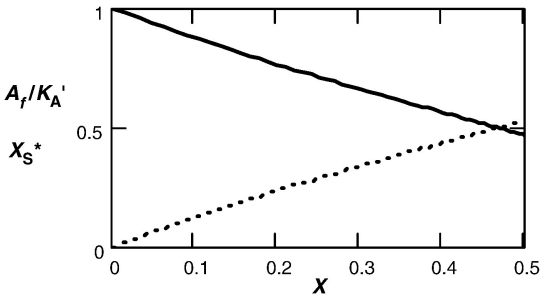


Fig. A1. The decrease in the free A concentration (solid line) with increasing total mole fraction of $S$, $X=S_T/(S_T+A_T)$, for $A_T=6$ mM and $K'_A=1.5$ mM. The dotted line shows the concomitant increase of the mole fraction of $S$ in the interface.

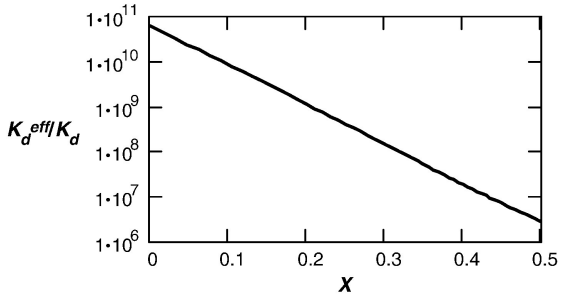


Fig. A2. The decrease in the effective dissociation constant for enzyme and interface with increasing total mole faction of SM in the system from Eq. (A5) with $A_T=6$ mM, $K'_A=1.5$ mM, $n_1=3$, $n_2=3.6$, $n_3=8.4$, $K_1=0.025$ mM, $K_2=0.2$ mM, and $K_3=0.8$ mM.

containing vesicles. In the diffusion limit, the exchange rate of enzyme between micelles will be on the order of (p. 37 in [4])

$$k_{exch}\sim 10^4 K_d^{eff} \quad \left(s^{-1} \text{ if } K_d^{eff} \text{ is in mM}\right)$$

This is an upper estimate and it is crucially dependent on the parameters that determine $K_d^{eff}$. The best fit to experimental data shown in Fig. 4 requires a much smaller numerical factor before $K_d^{eff}$; this suggests that enzyme exchange is not diffusion limited, which is not unexpected as both E* and $E_i^{\#}$ are tightly bound complexes and their interconversion is unlikely to be instantaneous. SMase binds tightly to SM vesicles and carries out reaction progress in the scooting mode. $K_d^{eff}$ is the effective destabilization of the E* state when A is available to form premicellar complexes. One effect of this destabilization is to decrease the amount of active enzyme (E*) thereby decreasing $v_i$. Another effect will be to increase the enzyme-exchange rate between the S+A mixed micelles.

If $K_d^{eff}$ is small, exchange will not be sufficiently fast and we need to consider that substrate will be depleted in each

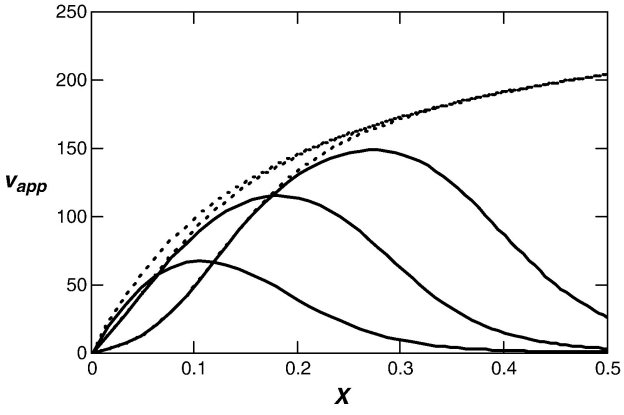


Fig. A3. Solid curves show the predicted enzyme rate from Eq. (A7) as function of total mole fraction of S in the system. Same parameter values as in Fig. A2 and $N_T=200$, $k_{cat}^*=300\ s^{-1}$, $K_M^*=0.25$ mole fraction, $k_{exch}=100\ K_d^{eff}\ s^{-1}$, and from upper to lower $K_d=10^{-9}$, $10^{-10}$, $10^{-11}$ mM. The dotted curves show the corresponding initial rates expected from Eq. (A6) when exchange is not limiting.

affected micelle during the residence time of the enzyme. Assuming at most one enzyme per micelle and with a possibly slow enzyme exchange, this gives an apparent initial rate (cf. pp. 119–120 in [4]):

$$v_{\mathrm{app}} = \frac{k^*_{\mathrm{cat}} X^*_{\mathrm{S}}}{K^*_{\mathrm{M}}\left(1 + K^{\mathrm{eff}}_{\mathrm{d}}/M^*\right) + k^*_{\mathrm{cat}}/\left(k_{\mathrm{exch}} N_{\mathrm{T}}\right) + X^*_{\mathrm{S}}} \qquad \text{(A7)}$$

Here, $N_T$ is the size of a micelle, i.e., the number of A and S molecules. $X_S$* is the initial mole fraction of substrate in a vesicle before depletion by enzyme (Eq. (A1)). The true initial rate would still be given by Eq. (A6), but it would be of short duration and the stationary-state rate in Eq. (A7) would appear to be an initial rate. The equation for $v_{app}$ gives the correct limit for fast exchange, $v_i$, Eq. (A6). In the limit of very slow exchange, Eq. (A7) gives $v_{app} = k_{exch} N_T X_S$*, which corresponds to the case when all $N_T X_S$* substrate molecules in each micelle are consumed before exchange takes place. Fig. A3 shows some results. At low mole fraction of S, there is more monodisperse A in solution so that exchange is relatively fast and Eq. (A6) suffices to describe the enzyme rate. In this region, the enzyme rate increases with increasing S both because of the increase in substrate concentration in the interface (increase in $X_S$*), and because of the tighter binding of enzyme to the interface (decrease in $K_d^{eff}$). At higher concentration of S, the enzyme rate becomes limited by the exchange rate as the concentration ($A_f$) of monodisperse amphiphile decreases.

In summary, these results are based on the assumptions that (i) mixing and partitioning in micelles is ideal, (ii) the partitioning is not influenced by bound enzyme and enzyme binding is not influenced by micelle composition, (iii) the size of the micelles is not influenced by the composition or by bound enzyme, and (iv) product inhibition does not contribute. Due to the cooperative nature of the premicellar complex formation, minor deviations from these assumptions could have large effects on $K_d^{eff}$ and $k_{exch}$ and thereby on the overall enzyme rate. Thus, deviations can be expected although the general trends seem to be well described (Fig. 4).

## References


[1] B.Z. Yu, D. Zakim, M.K. Jain, Processive interfacial catalytic turnover by *Bacillus cereus* sphingomyelinase on sphingomyelin vesicles, Biochim. Biophys. Acta 1583 (2002) 122–132.

[2] M.K. Jain, J. Rogers, D.V. Jahagirdar, J.F. Marecek, F. Ramirez, Kinetics of interfacial catalysis by phospholipase A2 in intravesicle scooting mode, and heterofusion of anionic and zwitterionic vesicles, Biochim. Biophys. Acta 860 (1986) 435–447.

[3] O.G. Berg, M.H. Gelb, M.D. Tsai, M.K. Jain, Interfacial enzymology: the secreted phospholipase A2-paradigm, Chem. Rev. 101 (2001) 2613–2654.

[4] O.G. Berg, M.K. Jain, Interfacial Enzyme Kinetics, Wiley, London, 2002.

[5] M.K. Jain, O.G. Berg, The kinetics of interfacial catalysis by phospholipase A2 and regulation of interfacial activation: hopping versus scooting, Biochim. Biophys. Acta 1002 (1989) 127–156.

[6] H.M. Verheij, A.J. Slotboom, G.H. de Haas, Structure and function of phospholipase A2, Rev. Physiol. Biochem. Pharmacol. 91 (1981) 91–203.

[7] O.G. Berg, B.Z. Yu, R.J. Apitz-Castro, M.K. Jain, Phosphatidylinositol-specific phospholipase C forms different complexes with monodisperse and micellar phosphatidylcholine, Biochemistry 43 (2004) 2080–2090.

[8] O.G. Berg, B.Z. Yu, C. Chang, K.A. Koehler, M.K. Jain, Cooperative binding of monodisperse anionic amphiphiles to the i-face: phospholipase A2-paradigm for interfacial binding, Biochemistry 43 (2004) 7999–8013.

[9] B.Z. Yu, R. Apitz-Castro, M.D. Tsai, M.K. Jain, Interaction of monodisperse anionic amphiphiles with the i-face of secreted phospholipase A2, Biochemistry 42 (2003) 6293–6301.

[10] T. Obama, Y. Kan, H. Ikezawa, M. Imagawa, K. Tsukamoto, Glu-53 of *Bacillus cereus* sphingomyelinase acts as an indispensable ligand of Mg2+ essential for catalytic activity, J. Biochem. (Tokyo) 133 (2003) 279–286.

[11] M. Tomita, R. Taguchi, H. Ikezawa, The action of sphingomyelinase of *Bacillus cereus* on bovine erythrocyte membrane and liposomes. Specific adsorption onto these membranes, J. Biochem. (Tokyo) 93 (1983) 1221–1230.

[12] R. Eksteen, K.J. Pardue, Modified silica-based packing materials for size exclusion chromatography, in: C. Wu (Ed.), Handbook of Size Exclusion Chromatography and Related Techniques, Marcel Dekker, Inc, New York, 2004, pp. 45–98.

[13] D. Marion, K. Wüthrich, Application of phase sensitive two-dimensional correlated spectroscopy (COSY) for measurements of 1H–1H spin–spin coupling constants in proteins, Biochem. Biophys. Res. Commun. 113 (1983) 967–974.

[14] F. Delaglio, S. Grzesiek, G.W. Vuister, G. Zhu, J. Pfeifer, A.A. Bax, NMRPipe: a multidimensional spectral processing system based on UNIX pipes, J. Biomol. NMR 6 (1995) 277–293.

[15] T.D. Goddard, D.G. Kneller, SPARKY-3, University of California, San Francisco.

[16] T.E. Polenova, T.A. Iwashita, G.I. Palmer, A.G. McDermott, Conformation of the trypanocidal pharmaceutical suramin in its free and bound forms: transferred nuclear overhauser effect studies, Biochemistry 36 (1997) 14202–14217.

[17] O.G. Berg, B.Z. Yu, J. Rogers, M.K. Jain, Interfacial catalysis by phospholipase A2: determination of the interfacial kinetic rate constants, Biochemistry 30 (1991) 7283–7297.

[18] M.K. Jain, B.Z. Yu, J. Rogers, G.N. Ranadive, O.G. Berg, Interfacial catalysis by phospholipase A2: dissociation constants for calcium, substrate, products, and competitive inhibitors, Biochemistry 30 (1991) 7306–7317.

[19] M.K. Jain, J. Rogers, H.S. Hendrickson, O.G. Berg, The chemical step is not rate-limiting during the hydrolysis by phospholipase A2 of mixed micelles of phospholipid and detergent, Biochemistry 32 (1993) 8360–8367.

[20] M.K. Jain, J. Rogers, O. Berg, M.H. Gelb, Interfacial catalysis by phospholipase A2: activation by substrate replenishment, Biochemistry 30 (1991) 7340–7348.

[21] O.G. Berg, J. Rogers, B.Z. Yu, J. Yao, L.S. Romsted, M.K. Jain, Thermodynamic and kinetic basis of interfacial activation: resolution of binding and allosteric effects on pancreatic phospholipase A2 at zwitterionic interfaces, Biochemistry 36 (1997) 14512–14530.

[22] Y. Cajal, O.G. Berg, M.K. Jain, Direct vesicle–vesicle exchange of phospholipids mediated by polymyxin B, Biochem. Biophys. Res. Commun. 210 (1995) 746–752.

[23] Y. Cajal, J. Rogers, O.G. Berg, M.K. Jain, Intermembrane molecular contacts by polymyxin B mediate exchange of phospholipids, Biochemistry 35 (1996) 299–308.

[24] C. Luberto, D.F. Hassler, P. Signorelli, Y. Okamoto, H. Sawai, E. Boros, D.J. Hazen-Martin, L.M. Obeid, Y.A. Hannun, G.K. Smith, Inhibition of tumor necrosis factor-induced cell death in MCF7 by a novel inhibitor of neutral sphingomyelinase, J. Biol. Chem. 277 (2002) 41128–41139.

[25] A.P. Campbell, B.D. Sykes, Theoretical evaluation of the two-dimensional transferred nuclear overhauser effect, J. Magn. Reson. 93 (1991) 77–92.

[26] M.E. Venable, J.Y. Lee, M.J. Smyth, A. Bielawska, L.M. Obeid, Role of ceramide in cellular senescence, J. Biol. Chem. 270 (1995) 30701–30708.

[27] Y.A. Hannun, C. Luberto, K.M. Hargraves, Enzymes of sphingolipid metabolism: from modular to integrative signaling, Biochemistry 40 (2001) 4893–4903.

[28] K. Hofmann, S. Tomiuk, G. Wolff, W. Stoffel, Cloning and characterization of the mammalian brain-specific, Mg2+-dependent neutral sphingomyelinase, Proc. Natl. Acad. Sci. U. S. A. 97 (2000) 5895–5900.

[29] F. Rodriguz-Lima, A.C. Fensome, M. Joesphs, J. Evans, R.J. Veldman, M. Katan, Structural requirements for catalysis and membrane targeting of mammalian enzymes from neutral sphingomyelinase and lysophospholipid phospholipase C activities., J. Biol. Chem. 275 (2000) 28316–28325.

[30] H. Ikezawa, M. Mori, T. Ohyabu, R. Taguchi, Studies on sphingomyelinase of *Bacillus cereus*. I. Purification and properties, Biochim. Biophys. Acta 528 (1978) 247–256.

[31] R.J. Tausk, J.T. Overbeek, Physical chemical studies of short-chain lecithin homologues: IV. A simple model for the influence of salt and the alkyl chain length on the micellar size, Biophys. Chem. 2 (1974) 175–179.

[32] R.J. Tausk, J. van Esch, J. Karmiggelt, G. Voordouw, J.T. Overbeek, Physical chemical studies of short-chain lecithin homologues. II. Micellar weights of dihexanoyl- and diheptanoyllecithin, Biophys. Chem. 1 (1974) 184–203.

[33] G.M. Carman, R.A. Deems, E.A. Dennis, Lipid signaling enzymes and surface dilution kinetics, J. Biol. Chem. 270 (1995) 18711–18714.

[34] P. Subramanian, R.V. Stahelin, Z. Szulc, A. Bielawska, W. Cho, C.E. Chalfant, Ceramide-1-phosphate acts as a positive allosteric activator of group IVA cytosolic phospholipase A2 alpha and enhances the interaction of the enzyme with phosphatidylcholine, J. Biol. Chem. 280 (2005) 17601–17607.